Materials Advances

ROYAL SOCIETY OF CHEMISTRY

PAPER

View Article Online
View Journal | View Issue

Cite this: *Mater. Adv.*, 2024, 5, 9000

Biocompatible and low-cost iodine-doped carbon dots as a bifunctional fluorescent and radiocontrast agent for X-ray CT imaging†

Timur Sh. Atabaev, *[a] Dinara Askar, [b] Zarina Baranchiyeva, [a] Balnur A. Zhainsabayeva, [a] Timur Elebessov, [b] Moon Sung Kang, [c] Bakyt Duisenbayeva, [d] Ellina A. Mun, *[a] Tri Thanh Pham *[b] and Dong-Wook Han *[c]

Carbon dot-based radiocontrast agents have recently sparked the interest of researchers owing to their better contrasting capabilities, simple synthesis protocols, high colloidal stability, and good biocompatibility. In this study, we propose for the first time the synthesis of iodine-doped carbon dots (I-CDs) using low-cost reagents such as citric acid ($C_6H_8O_7$), urea (CH_4N_2O) and potassium iodide (KI). The as-prepared I-CDs demonstrated excellent colloidal stability (with a zeta potential value of −64.7 mV), excitation-dependent fluorescent properties (with a maximum quantum yield of ∼8.9%), and a mean iodine concentration of ∼4.67 wt%. Notably, the as-prepared I-CDs displayed greater X-ray attenuation efficiency (42.87 HU mL mg^{-1}) as compared to the commercially employed iopromide radiocontrast agent (30.98 HU mL mg^{-1}). Furthermore, ATPase activity, cytotoxicity analysis with HeLa, NHDF, HEK293, and A549 cell lines, and live-cell imaging experiments of the *Drosophila* neuroblasts in intact brain lobes suggested high biocompatibility and nontoxicity of the prepared I-CDs. Overall, biocompatible and low-cost I-CDs show great promise as bifunctional radiocontrast and fluorescent agents for biomedical applications.

Received 14th August 2024,
Accepted 16th October 2024

DOI: 10.1039/d4ma00823e

rsc.li/materials-advances

1. Introduction

Computed tomography (CT) is a non-invasive imaging and diagnostic tool widely employed in medicine. Iodinated organic radiocontrast agents are widely employed during CT scans to improve contrast between nearby tissues, facilitating more reliable imaging of diseased regions.[1] The administration of iodinated radiocontrast agents is considered to be a safe procedure, with mild itching or cutaneous reactions as the most common side effects. However, there are also serious complications such as delayed allergic reactions, anaphylactic reactions, and acute renal injury.[2–4] Therefore, the search for biocompatible CT radiocontrast agents with high contrasting properties is considered as an urgent and pressing issue in the healthcare sector.

Carbon dots (CDs) doped with various metals have been presented as a viable solution to the aforementioned issues owing to their nontoxicity, excellent colloidal stability, fabrication simplicity, and distinctive optical properties suitable for bioimaging purposes. In principle, a wide range of dopants can be incorporated into the CD matrix to achieve excellent radiocontrast characteristics, although iodine and lanthanide elements are the most effective for CT X-ray attenuation.[5] For example, Zhao *et al.*[6] prepared gadolinium (Gd), and ytterbium (Yb) codoped CDs with X-ray attenuation efficiency of 45.43 HU L g^{-1} (where HU – Hounsfield units), which was higher as compared to clinical iobitridol (31.83 HU L g^{-1}). Bouzas-Ramos and colleagues[7] also reported that the X-ray attenuation efficiency of Gd and Yb-codoped CDs (14.4 HU mM^{-1}) was higher as compared to iobitridol (5.0 HU mM^{-1}). The X-ray attenuation efficiency of manganese (Mn) and dysprosium (Dy) codoped CDs[8] was found to be ∼47.34 HU L g^{-1}, while bismuth (Bi) and Gd codoped CDs attained a value of ∼164.66 HU L g^{-1}.[9] In our recent study, we demonstrated that terbium (Tb)-doped CDs can achieve the X-ray attenuation efficiency of ∼48.2 HU L g^{-1}, which is comparable to that of double element co-doped systems.[6,8] Despite these encouraging findings, the use of

[a] *Department of Chemistry, Nazarbayev University, Astana 010000, Kazakhstan. E-mail: timur.atabaev@nu.edu.kz, ellina.mun@nu.edu.kz*
[b] *Department of Biology, Nazarbayev University, Astana 010000, Kazakhstan. E-mail: tri.pham@nu.edu.kz*
[c] *Department of Cogno-Mechatronics Engineering, Pusan National University, Busan 46241, Republic of Korea. E-mail: nanohan@pusan.ac.kr*
[d] *Department of Radiology, Republican Diagnostic Center, Astana 010000, Kazakhstan*

† Electronic supplementary information (ESI) available. See DOI: https://doi.org/10.1039/d4ma00823e

lanthanides is still deemed costly and unsustainable due to their scarcity and uneven distribution in the Earth's crust. As a result, attempts have been made to switch from lanthanides to other more abundant elements having appropriate K-edge values, such as hafnium (Hf), barium (Ba), and iodine (I). Typically, Hf-doped CDs[10] and Ba-CDs[11] achieved X-ray attenuation efficiency values of 7.21 HU mM^{-1} and 13.2 HU mM^{-1}, respectively. To date, only three studies have reported on the synthesis and radiocontrast properties of I-doped CDs.[12–14] M. Zhang and colleagues[12] employed a hydrothermal process using glycine and iodixanol (a commercial contrast agent) to produce I-doped CDs. H. Su and co-authors[13] utilized citric acid and iohexol (a commercial contrast agent) as precursors for the synthesis of cetuximab-conjugated I-CQDs. In a similar manner, Y. Jeong and colleagues used lactobionic acid and iohexol to produce I-doped CDs.[14] Although all of these I-doped CDs had better contrasting properties as compared to clinically used iodine-based contrast agents (iohexol and iodixanol), specific X-ray attenuation efficiency values were not determined/reported in all three studies. However, the attenuation efficiency value is an important parameter and frequently reported to compare with other developed radiocontrast agents. Moreover, producing I-CDs from commercial iodine contrast agents appears to be economically unfeasible. Hence, the main objective of this research is to prepare I-CDs from low-cost reagents like citric acid ($C_6H_8O_7$), urea (CH_4N_2O), and potassium iodide (KI) and to study their radiocontrasting properties. We showed that the prepared I-CDs have better contrasting properties as compared to the commercial iopromide contrast agent, and a plausible contrast enhancement mechanism is proposed. Lastly, an extensive toxicity study with several cell lines suggested the good biocompatibility of the prepared I-CDs.

2. Materials and methods

2.1. Synthesis of I-CDs

High purity reagents were purchased from Merck and used as received. In a typical synthesis, citric acid (200 mg), urea (100 mg), and KI (10 mg) were dissolved in 10 mL of deionized (DI) water. Next, the mixture was transferred into a Teflon-lined hydrothermal reactor with capacity of 25 mL, sealed, and heated at 200 °C for 12 h. The resulting dark solution was filtered using Whatmann® filter paper to remove big precipitates, followed by a 0.1 μm syringe filter to remove submicron particles. The as-prepared solution was dialyzed in DI water for 36 hours, with a 12-hour interval between water changes. Finally, the purified I-CDs were freeze-dried for further usage and characterization. The obtained mass of the I-CDs was measured to be ~58.6 mg.

2.2. Characterization of I-CDs

The morphology of the as-prepared I-CDs was examined using transmission electron microscopy (TEM, Talos F200X G2, Thermo Fisher Scientific Inc.) operating at 200 kV. For sample analysis, a diluted solution of I-CDs with a concentration of 1 mg/10 mL in DI water was prepared first. Next, 1 μL of I-CD solution was dropped on a Formvar/carbon supported copper grid (400 mesh) and then dried for several hours under a glass cover. The functional groups analysis of I-CDs was performed by Fourier-transform infrared vibrational spectroscopy (FTIR, Nicolet iS5, Thermo Fisher Scientific Inc.) and by X-ray photoelectron spectroscopy (MultiProbe XPS, Scienta Omicron), respectively. Dynamic light scattering (DLS) and zeta potential magnitude were measured using a Nanotrac Wave II Q (Microtrac MRB). Zeta potential values of I-CDs have been measured in DI water (pH = 7.6) and phosphate-buffered saline (pH = 7.4) solution. The iodine content was quantified using inductively coupled plasma optical emission spectroscopy (ICP-OES) (iCAP 6300 duo, Thermo Fisher Scientific Inc.). Optical properties and absolute quantum yield measurements of I-CDs have been performed using an RF 6000 spectrofluorophotometer (Shimadzu Corp.) and Quantaurus C9920-02 absolute quantum yield spectrophotometer (Hamamatsu Photonics K.K.). X-ray attenuation measurements were tested using a Philips Brilliance 64 (Koninklijke Philips N.V.) clinical computed tomography (CT) instrument. Phantom images were acquired using standard CT parameters: X-ray tube voltage = 120 kV and field of view (FOV) = 120 mm.

2.3. Biosafety of I-CDs

All experimental methods used to determine the ATPase activity, cytotoxicity, and live-cell imaging of intact *Drosophila* brain lobes are described in the ESI.†

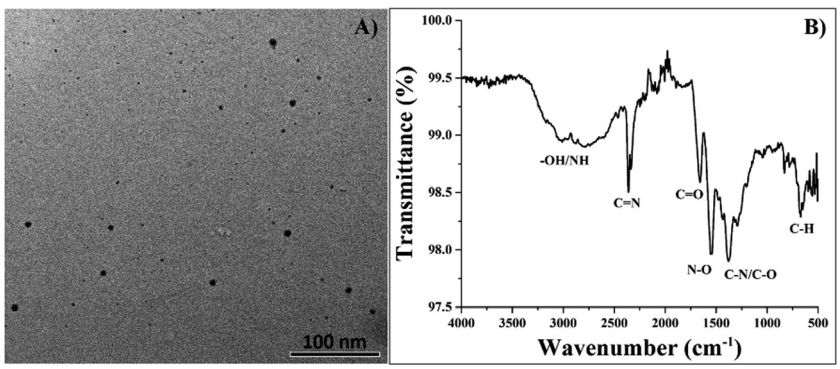

Fig. 1 (A) HR-TEM image and (B) FTIR analysis of the prepared I-CDs.

3. Results and discussion

3.1. TEM, FTIR and XPS analyses of I-CDs

The carbonization of organic molecules in the presence of KI allows for the incorporation of iodine into the carbon core, resulting in the formation of I-CDs. Fig. 1a shows a TEM image of prepared I-CDs with the corresponding size distribution. One can easily observe the formation of quasi-spherical carbon dots with average sizes of $\sim 10 \pm 4$ nm and a polydispersity index (PDI) value of 1.19 according to dynamic light scattering (DLS) results depicted in Fig. S1 (ESI†). Visual observation of the colloidal solution and zeta potential studies suggests that I-CDs have good colloidal stability, with a zeta potential value of around (−64.7 mV) in DI water and (−47.1 mV) in PBS buffer. Fig. 1b shows the results of FTIR analysis of the prepared I-CDs. A broad band between 2800 and 3300 cm^{-1} can be assigned to hydroxyl group/H-bonded OH stretch and primary amine NH stretch vibrations.[15] Two bands at 2240 cm^{-1} and 1735 cm^{-1} correspond to C═N and C═O stretch vibrations, respectively. A band at 1510 cm^{-1} can be assigned to N–O asymmetric stretch, whereas the band at 1310 cm^{-1} can be attributed to C–N/C–O stretch vibrations.[15] A C–H bend vibration can also be observed at 610 cm^{-1}.[15] Hence, it is reasonable to expect that the prepared I-CDs have a substantial amount of functional groups (carbonyl, amino, hydroxyl, *etc.*) on their surfaces, which also helps to explain the excellent colloidal stability of I-CDs in aqueous solution.

Next, the sample was tested using XPS to validate the incorporation of iodine elements into CDs. Fig. 2 depicts a full-range XPS survey with four easily detectable signals representing I 3d, O 1s, N 1s, and C 1s. Generally, only carbon and iodine elements can substantially influence the degree of X-ray attenuation; hence, only these two elements underwent in-depth XPS investigation. The high-resolution spectra of the C 1s band can be deconvoluted into three main peaks at 284.8, 279.8, and 291.3 eV featuring the presence of C–C/C═C, C–N/C–O, and C═N/C═O groups, respectively.[13] High-resolution spectra of I 3d revealed the presence of I $3d_{5/2}$ and $3d_{3/2}$ doublets at 618.2 and 629.6 eV, respectively. Hence, XPS survey confirmed that negatively charged iodine (I^-) exists in the I-CD structure.[12,13] On the other hand, two additional I $3d_{5/2}$ and $3d_{3/2}$ doublets at $\sim$ 626.3 eV and 636.1 eV suggest that neutral iodine molecules (I_2) are likely tightly absorbed on the surface defect locations of I-CDs.[12] The mean total iodine concentration in the I-CDs was estimated to be $\sim$4.67 wt%.

3.2. Fluorescence properties of I-CDs

Next, the excitation-dependent optical properties of the I-CDs were examined using a spectrofluorophotometer. Fig. S2 (ESI) indicates that the produced I-CDs have excitation-dependent optical properties, with the most effective excitation range between 400–420 nm. The emission range with optimal excitation covers nearly the entire visible spectrum ($\sim$400–670 nm) with the most intense signal in the blue-green area. The excitation-dependent emission feature of the I-CDs further confirms the presence of surface defects, multiple functional groups on the surface, and polydispersity of I-CDs. In particular, blue emission is commonly attributed to surface defect fluorescence,[16] whereas green emission arises from surface functional groups (carbonyl/carboxyl, *etc.*).[17] The maximum absolute quantum yield (QY) for I-CDs has been estimated to be 8.9% at 410 nm excitation, which is comparable to most CDs reported to date. High Stokes shift and excellent colloidal stability make these I-CDs promising as green light emitting fluorescent tags in biomedical studies.[18,19] For example, I-CDs incubated with HEK293 and A549 cells for 24 hours produce bright green fluorescence, whereas untreated cells show few green fluorescent specks due to autofluorescence, as shown in Fig. 3. The results also revealed that A549 cells absorbed I-CDs substantially better than HEK293 cells, which is most likely owing to differences in the morphologies and mechanical properties between the healthy and cancer cell lines. Furthermore, I-CDs rarely appear in the nucleus and are primarily found in the cytoplasm. It should be noted that no treatments such as fixation or permeabilization were used, emphasizing the great potential of I-CDs for fluorescent labeling of live cells, particularly the cytoplasmic components of cancer cells, where I-CDs are most absorbed.

3.3. X-ray attenuation efficiency of I-CDs

Clinical CT was used to evaluate the X-ray attenuation efficiency of the developed I-CDs, iopromide (Ultravist), and pure CDs (without the iodine element). Hounsfield unit (HU) values for I-CDs and iopromide were determined at iodine concentrations ranging from 0 to 2 mg mL^{-1} (HU for DI water = 0). Fig. 4

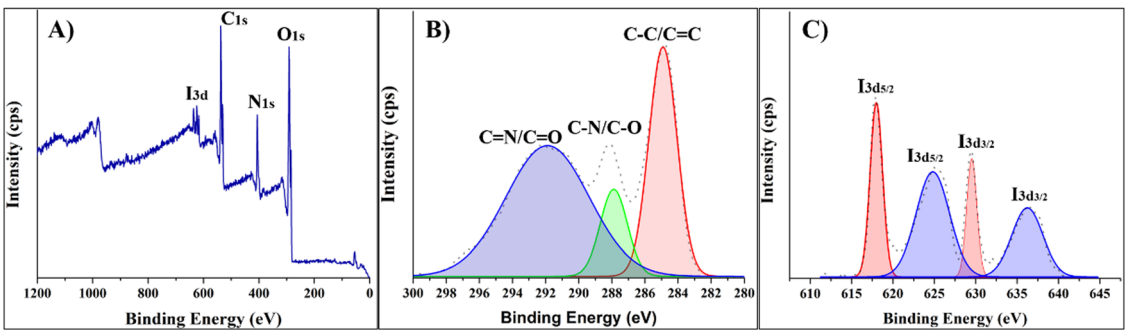

Fig. 2 (A) The XPS full scan of I-CDs. High-resolution XPS scans of (B) C 1s and (C) I 3d.

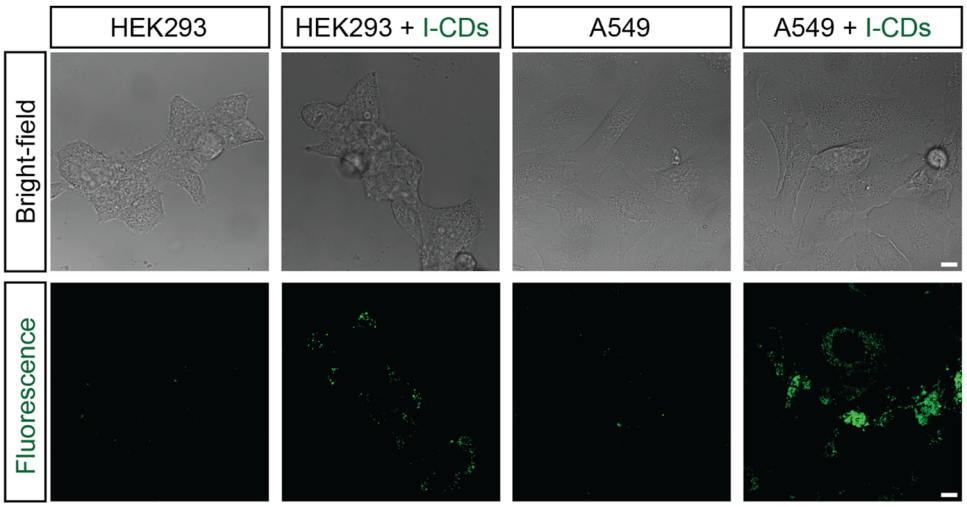

Fig. 3 Bright-field and fluorescent images of HEK293 and A549 cells without and with I-CDs (5000 ppm) after 24 hours of incubation. The scale bar is 5 microns.

reveals that I-CDs had a higher X-ray attenuation efficiency (~42.87 HU mL mg^{-1}) than commercial iopromide contrast agent (~30.98 HU mL mg^{-1}) at equivalent iodine concentration. Interestingly, available literature on I-doped CDs[12–14] has yielded no information about the contrast enhancement mechanism. We speculated that bare CDs can also attenuate X-rays to some extent and measured the X-ray attenuation efficiency of pure CDs (by taking into consideration the weight percent of iodine in a given I-CD concentration). The results indicate that bare CDs could also attenuate X-rays with an efficiency of ~11.24 HU mL mg^{-1}, explaining clearly the attenuation efficacy difference between I-CDs and iopromide. Thus, one can assume that the prepared I-CDs yielded a better efficacy thanks to synergetic X-ray attenuation by the iodine element and CDs. It should also be noted that the equivalent mass of I-CDs required to obtain a reasonable contrast *in vivo* should be several times higher depending on iodine concentration in iopromide or any other iodine-based commercial contrast agent. However, previous studies[12,14] revealed that I-CDs are better tolerated and provide higher contrast *in vivo* than iodine-based contrast agents, even at relatively high concentrations of up to 10 mg mL^{-1}.

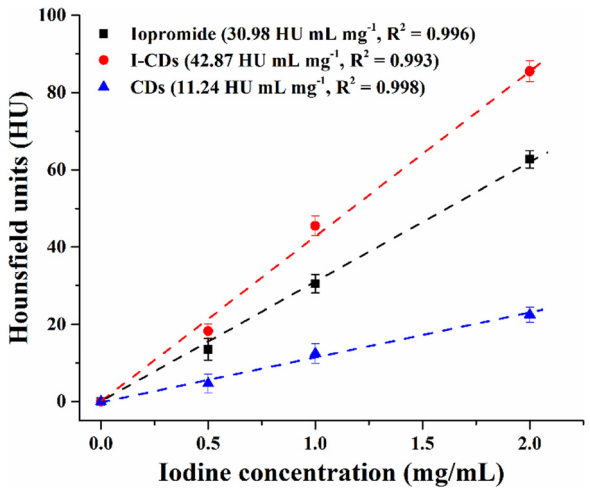

Fig. 4 The measured CT values of I-CDs and iopromide as a function of iodine concentration. Bare CD concentrations were taken based on the actual I-CD concentration (without iodine mass).

3.4. Non-toxicity of I-CDs to insect and mammalian cells

To ensure that I-CDs did not have any cytotoxic effects on the cells, we first assessed the ATPase enzymatic activity of I-CDs at different concentrations. ATPase activity has been shown to increase actomyosin contractility, resulting in the collapse of the actin cytoskeleton cortex and cell death.[20] Thus, assessing ATPase activity will provide insight into how toxic I-CDs are to cells and how they affect cell division. To test this, I-CDs were incubated at room temperature for 30 minutes with 1 mM ATP. The ATPase reaction was terminated by adding 200 μL of malachite green assay reagent, resulting in a colorimetric product. Absorbance values from this product clearly indicate that I-CDs do not have ATPase activity at the treated concentration (50 ppm) or at concentrations several times higher (Fig. S3 and Table S1, ESI†). Even at extremely high concentrations, such as 10 000 ppm, ATPase activity only increases by about 3%. Furthermore, the overall ATPase activity value is less than 1 nM min^{-1} μL^{-1}, which is extremely low and will have no effect on the cell. The fact that the treated concentration of I-CDs has no effect on cell viability or proliferation makes it generally considered safe for human use.

Time-lapse or live-cell imaging of the brain over a 3-hour period in 3rd instar *Drosophila* larval brain was carried out to measure the number of neuroblast divisions during this period in order to test the cytotoxicity of I-CDs on *Drosophila* neuroblasts in intact brain. This live cell imaging technique allows us to observe the number of divisions as well as the dynamic changes in cell size and shape over time. To ensure that neuroblasts in intact brains will receive comparable exposure

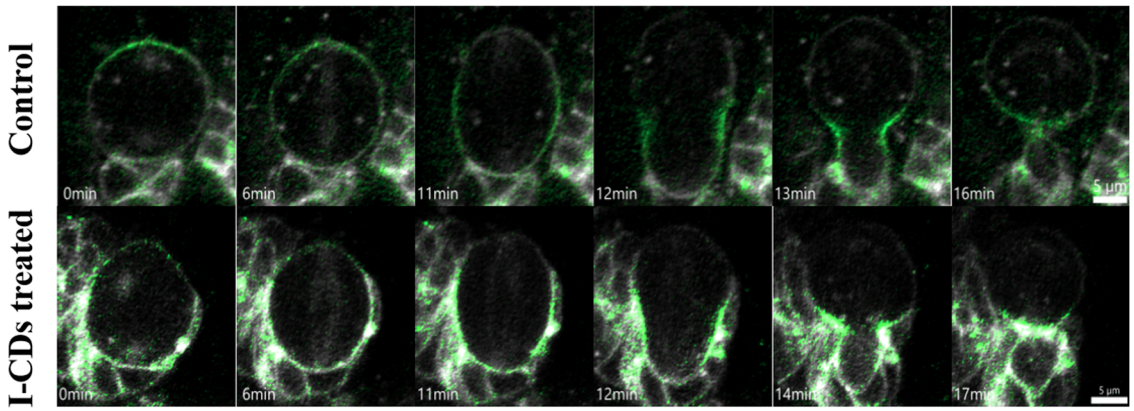

Fig. 5 Image sequences of a *Drosophila* neuroblast dividing in an intact brain. The top row shows the normal asymmetric cell division of a control neuroblast. The bottom row depicts normal asymmetric cell division of a 200 ppm of I-CDs treated neuroblast. Non-muscle myosin 2 is shown in green, with the cell membrane and spindle in white. The scale bar measures 5 microns in length.

to I-CDs as isolated cells in culture, the glial blood–brain barrier of the brain lobes was dissociated by incubating with collagenase type I for 10 minutes. Fig. 5 shows that neither the control nor the I-CD-treated brains displayed any abnormal activity during mitosis, suggesting that I-CDs may not be cytotoxic to *Drosophila* neural stem cells. In order to assess how I-CDs affect neuroblasts' ability to proliferate in an intact brain, the number of cell divisions during a 3-hour live cell imaging session was evaluated (Fig. S4, ESI†). The results clearly demonstrated that there was no noticeable difference in the number of neuroblast divisions between the brains treated with two different I-CD concentrations, 50 ppm and 200 ppm, and the control group. This data further supports that I-CDs are not cytotoxic to *Drosophila* neural stem cells.

The biocompatibility of the developed I-CDs was also assessed using the standard MTT assay in two different locations (South Korea and Kazakhstan). Fig. 6 and Fig. S5 (ESI†) show the dose-dependent viability profiles of HEK293, A549, NHDF, and HeLa cells in the presence of I-CDs with concentrations ranging from 0.2 to 200 μg mL^{-1}. One can notice that I-CDs exhibit no signs of toxicity in all cases, indicating their good *in vitro* biocompatibility according to the ISO 10993-5 standard.[21] On the other hand, different cells may react differently to as-prepared I-CDs,[22] hence, additional biocompatibility studies need to be conducted. Further research is also needed to understand the circulatory mechanism and probable accumulation of I-CDs in vital organs. Moreover, emission color switching[23–26] or excitation-independent emission[27–29] of CDs can be realized by introducing/coupling with other elements that can be relevant for bioimaging applications. These questions can be addressed in forthcoming studies.

4. Conclusion

In this study, I-doped CDs were produced from low-cost reagents such as citric acid, urea, and potassium iodide, as opposed to previously employed clinical iodine contrast agents as starting precursors. CT X-ray attenuation results confirmed that the prepared I-CDs demonstrate better efficacy (42.87 HU mL mg^{-1}) as compared to iopromide contrast agent (30.98 HU mL mg^{-1}) at equal iodine concentration. The

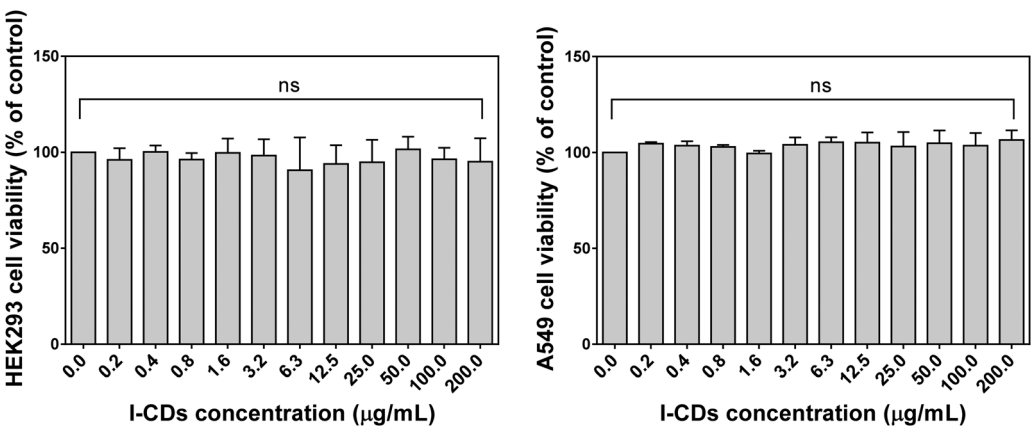

Fig. 6 Effects of I-CDs on the viability of HEK293 and A549 cell lines after 24 hours (p value < 0.005).

plausible mechanism for contrasting property enhancement is bare CD-induced partial X-ray attenuation, which is confirmed by X-ray attenuation measurements. Preliminary biosafety assessments verified the good biocompatibility of the produced I-CDs; nevertheless, additional study is still required to determine the fate of I-CDs in the circulatory system of small animal models and their potential accumulation in vital organs. Nonetheless, the low production cost and improved contrasting properties make I-CDs promising candidates for application as fluorescent and CT contrast agents.

Data availability

The data supporting this article have been included as part of the ESI.†

Author contributions

The manuscript was written through contributions from all authors. All authors have given approval to the final version of the manuscript.

Conflicts of interest

The authors declare no competing financial interest.

Acknowledgements

This research was funded by the Science Committee of the Ministry of Science and Higher Education of the Republic of Kazakhstan (Grant No. AP19578878). This work was also partially supported by the Collaborative Research Program (Grant No. 021220CRP0522), Nazarbayev University, Kazakhstan.

References

1 M. V. Spampinato, A. Abid and M. G. Matheus, Current radiographic iodinated contrast agents, *Magn. Reson. Imaging Clin. N. Am*, 2017, **25**, 697–704.
2 M. Andreucci, T. Faga, R. Serra, G. De Sarro and A. Michael, Update on the renal toxicity of iodinated contrast drugs used in clinical medicine, *Drug, Healthcare Patient Saf.*, 2017, **9**, 25–37.
3 A.-L. Faucon, G. Bobrie and O. Clément, Nephrotoxicity of iodinated contrast media: From pathophysiology to prevention strategies, *Eur. J. Radiol.*, 2019, **116**, 231–241.
4 A. Kistner, C. Tamm, A. M. Svensson, M. O. Beckman, F. Strand, M. Sköld and S. Nyrén, Negative effects of iodine-based contrast agent on renal function in patients with moderate reduced renal function hospitalized for COVID-19, *BMC Nephrol.*, 2021, **22**, 297.
5 A. Molkenova, T. S. Atabaev, S. W. Hong, C. Mao, D.-W. Han and K. S. Kim, Designing inorganic nanoparticles into computed tomography and magnetic resonance (CT/MR) imaging-guidable photomedicines, *Mater. Today Nano*, 2022, **18**, 100187.
6 Y. Zhao, X. Hao, W. Lu, R. Wang, X. Shan, Q. Chen, G. Sun and J. Liu, Facile preparation of double rare earth-doped carbon dots for MRI/CT/FI multimodal imaging, *ACS Appl. Nano Mater.*, 2018, **1**, 2544–2551.
7 D. Bouzas-Ramos, J. C. Canga, J. C. Mayo, R. M. Sainz, J. R. Encinar and J. M. Costa-Fernandez, Carbon quantum dots codoped with nitrogen and lanthanides for multimodal imaging, *Adv. Funct. Mater.*, 2019, **29**, 1903884.
8 C. Li, Y. Wang, H. Nong, X. Hu, Y. Wu, Y. Zhang, C. Liang and K. Chen, S. Li. Manganese and dysprosium codoped carbon quantum dots as a potential fluorescent/T_1/T_2/CT quadri-modal imaging nanoprobe, *Nanotechnology*, 2021, **33**, 025101.
9 A. Molkenova, L. Serik, A. Ramazanova, K. Zhumanova, B. Duisenbayeva, A. Zhussupbekova, K. Zhussupbekov, I. V. Shvets, K. S. Kim, D. W. Han and T. S. Atabaev., Terbium-doped carbon dots (Tb-CDs) as a novel contrast agent for efficient X-ray attenuation, *RSC Adv.*, 2023, **13**, 14974–14979.
10 Y. Su, S. Liu, Y. Guan, Z. Xie, M. Zheng and X. Jing., Renal clearable hafnium-doped carbon dots for CT/Fluorescence imaging of orthotopic liver cancer, *Biomaterials*, 2020, **255**, 120110.
11 A. Molkenova, M. Kairova, A. Zhussupbekova, K. Zhussupbekov, B. Duisenbayeva, I. V. Shvets and T. S. Atabaev, Carbon dots doped with barium as a novel contrast agent for efficient CT X-ray attenuation, *Nano-Struct. Nano-Objects*, 2022, **29**, 100839.
12 M. Zhang, H. Ju, L. Zhang, M. Sun, Z. Zhou, Z. Dai, L. Zhang, A. Gong, C. Wu and F. Du, Engineering iodine-doped carbon dots as dual-modal probes for fluorescence and X-ray CT imaging, *Int. J. Nanomed.*, 2015, **10**, 6943–6953.
13 H. Su, Y. Liao, F. Wu, X. Sun, H. Liu, K. Wang and X. Zhu, Cetuximab-conjugated iodine doped carbon dots as a dual fluorescent/CT probe for targeted imaging of lung cancer cells, *Colloids Surf., B*, 2018, **170**, 194–200.
14 Y. Jeong, M. Jin, K. S. Kim and K. Na, Biocompatible carbonized iodine-doped dots for contrast-enhanced CT imaging, *Biomater. Res.*, 2022, **26**, 27.
15 J. Coates. Interpretation of infrared spectra, a practical approach in *Encyclopedia of Analytical Chemistry* ed. R. A. Meyers, John Wiley & Sons Ltd, Chichester, 2000, pp. 10815–10837.
16 P. Zhu, K. Tan, Q. Chen, J. Xiong and L. Gao, Origins of efficient multiemission luminescence in carbon dots, *Chem. Mater.*, 2019, **31**, 4732–4742.
17 L. Wang, S.-J. Zhu, H.-Y. Wang, S.-N. Qu, Y.-L. Zhang, J.-H. Zhang, Q.-D. Chen, H.-L. Xu, W. Han, B. Yang and H.-B. Sun, *ACS Nano*, 2014, **8**, 2541–2547.
18 Z. Zhu, Q. Li, P. Li, X. Xun, L. Zheng, D. Ning and M. Su, Surface charge controlled nucleoli selective staining with nanoscale carbon dots, *PLoS One*, 2019, **14**, e0216230.
19 A. Molkenova, A. Toleshova, S.-J. Song, M. S. Kang, A. Abduraimova, D.-W. Han and T. S. Atabaev, Rapid synthesis of nontoxic and photostable carbon nanoparticles for bioimaging applications, *Mater. Lett.*, 2020, **261**, 127012.

20 P. Cossio and G. M. Hocky, Catching actin proteins in action, *Nature*, 2022, **611**, 241–243.
21 https://nhiso.com/wp-content/uploads/2018/05/ISO-10993-5-2009.pdf.
22 Y. Y. Liu, Z. X. Sun, J. Liu, Q. Zhang, Y. Liu, A. Cao, Y. P. Sun and H. Wang, On the cellular uptake and exocytosis of carbon dots - significant cell type dependence and effects of cell division, *ACS Appl. Bio Mater.*, 2022, **5**, 4378–4389.
23 L. Jiang, H. Ding, S. Lu, T. Geng, G. Xiao and B. Zou, H. Bi. Photoactivated fluorescence enhancement in F,N-doped carbon dots with piezochromic behavior, *Angew. Chem., Int. Ed.*, 2020, **59**, 9986–9991.
24 L. Jiang, H. Ding, M. Xu, X. Hu, S. Li, M. Zhang, Q. Zhang, Q. Wang, S. Lu, Y. Tian and H. Bi, UV-Vis-NIR full-range responsive carbon dots with large multiphoton absorption cross sections and deep-red fluorescence at nucleoli and in vivo, *Small*, 2020, **16**, 2000680.
25 H. Ding, J. Xu, L. Jiang, C. Dong, Q. Meng, S. U. Rehman, J. Wang, Z. Ge, V. Y. Osipov and H. Bi, Fluorine-defects induced solid-state red emission of carbon dots with an excellent thermosensitivity, *Chin. Chem. Lett.*, 2021, **32**, 3646–3651.
26 J. Huang, C. Dong, J. Xu, J. Xuan, Q. Cheng and H. Bi, Nitrogen and chlorine co-doped carbon dots with synchronous excitation of multiple luminescence centers for blue-white emission, *New J. Chem.*, 2021, **45**, 7056–7059.
27 Y. Dong, H. Pang, H. B. Yang, C. Guo, J. Shao, Y. Chi, C. M. Li and T. Yu, Carbon-based dots co-doped with nitrogen and sulfur for high quantum yield and excitation-independent emission, *Angew. Chem., Int. Ed.*, 2013, **52**, 7800–7804.
28 G. M. Saladino, N. I. Kilic, B. Brodin, B. Hamawandi, I. Yazgan, H. M. Hertz and M. S. Toprak, Carbon quantum dots conjugated rhodium nanoparticles as hybrid multimodal contrast agents, *Nanomaterials*, 2021, **11**, 2165.
29 A. Mikhraliieva, V. Zaitsev, Y. Xing, H. Coelho-Júnior and R. L. Sommer, Excitation-independent blue-emitting carbon dots from mesoporous aminosilica nanoreactor for bioanalytical application, *ACS Appl. Nano Mater.*, 2020, **3**, 3652–3664.